5220 *Inorg. Chem.* **1992**, *31*, 5220–5225

Dialkoxyosmium(IV) Porphyrins. Crystal and Molecular Structures of Diethoxy-, Diphenoxy-, and Bis(2-propanolato)(*meso*-tetraphenylporphyrinato)osmium(IV)

Chi-Ming Che,*,† Jie-Sheng Huang,† Zao-Ying Li,† Chung-Kwong Poon,† Wai-Fong Tong,† Ting-Fong Lai,† Ming-Chu Cheng,‡ Chih-Chieh Wang,‡ and Yu Wang‡

Departments of Chemistry, The University of Hong Kong, Pokfulam Road, Hong Kong, and National Taiwan University, Taipei, Taiwan

Received February 6, 1992

A series of dialkoxyosmium(IV) porphyrins $[Os(Por)(OR)_2]$ [Por = TPP (*meso*-tetraphenylporphyrinato dianion), $(MeO)_{12}TPP$ (*meso*-tetrakis(3,4,5-trimethoxyphenyl)porphyrinato dianion); R = Me, Et, *i*-Pr, $PhCH_2$] were synthesized by treatment of $[Os(Por)(N_2)(THF)]$ [Por = TPP, $(MeO)_{12}TPP$] with alcohols in tetrahydrofuran (THF). All these new complexes were characterized by UV–visible, IR, and ^1H NMR spectroscopy. The X-ray crystal structures of $[Os(TPP)(OEt)_2]$, $[Os(TPP)(OCH(CH_3)_2)_2]$, and $[Os(TPP)(OPh)_2]$ have been determined: $[Os(TPP)(OEt)_2]$, monoclinic $P2_1/c$, $a = 9.858$ (1) Å, $b = 15.646$ (4) Å, $c = 13.137$ (2) Å, $\beta = 106.94$ (1)°, $Z = 2$; $[Os(TPP)(OCH(CH_3)_2)_2]$, triclinic $P\bar{1}$, $a = 9.812$ (1) Å, $b = 11.093$ (1) Å, $c = 11.656$ (1) Å, $\alpha = 70.83$ (1)°, $\beta = 76.08°$, $\gamma = 62.06$ (1)°, $Z = 1$; $[Os(TPP)(OPh)_2]$, triclinic $P\bar{1}$, $a = 10.253$ (1) Å, $b = 10.724$ (1) Å, $c = 11.958$ (1) Å, $\alpha = 62.08$ (1)°, $\beta = 68.55$ (1)°, $\gamma = 79.30$ (1)°, $Z = 1$. The RO–Os–OR axes in all complexes are required to be linear by symmetry with Os–OR distances ranging from 1.909 (4) to 1.938 (2) Å, indicating the presence of $d\pi(Os)$–$p\pi(O)$ interactions. The Os–O–C angles for the three complexes are nearly the same, being 127.0 (3)–128.2 (5)°.

Introduction

The monomeric dialkoxyosmium(IV) porphyrins have received considerable attention.[1,2] These osmium porphyrins are found to be paramagnetic, having similar μ_{eff} values as that found for six-coordinated d^4 metal–oxo complexes. However, a discrepancy between μ_{eff} of $[Os(OEP)(OMe)_2]$ (OEP = octaethylporphyrinato dianion) and $[Os(TPP)(OR)_2]$ was observed.[1b] In $[Os(OEP)(OMe)_2]$, the unusually low μ_{eff} value was thought to be due to the bending of the CH_3O–Os–OCH_3[1b] or Os–O–CH_3 axis,[2] which may lead to the splitting of the d_{xz}, d_{yz} orbitals and thus results in a very low energy triplet excited state. In order to understand the electronic structure of dialkoxyosmium(IV) porphyrins, it is essential to perform an X-ray structure determination. This is because the iterative extended Huckel (IEH) method, which has been used to calculate the electronic states of $[Os(OEP)(OMe)_2]$,[2] was based on presumed bond distances and angles. When measured bond distances and angles are used, the IEH calculation should be more convincing. Here we report the X-ray structure determinations on diethoxy-, diphenoxy-, and bis(2-propanolato)(*meso*-tetraphenylporphyrinato)osmium(IV). As far as we are aware, this is the first X-ray structural report on the monomeric d^4 dialkoxymetalloporphyrins. The synthesis and characterization of some new dialkoxyosmium(IV) porphyrins are also described.

Experimental Section

Materials. Dodecacarbonyltriosmium $[Os_3(CO)_{12}]$ was purchased from Strem Co. Ltd. *meso*-Tetraphenylporphyrin (H_2TPP) and *meso*-tetrakis(3,4,5-trimethoxyphenyl)porphyrin $[H_2(MeO)_{12}TPP]$ were prepared by the literature method.[3] The dinitrogenosmium(II) porphyrins $[Os(TPP)(N_2)(THF)]$ and $[Os(MeO)_{12}TPP(N_2)(THF)]$ were prepared by the method as described by Buchler and co-workers for the preparation of $[Os(OEP)(N_2)(THF)]$.[4]

$[Os^{IV}(Por)(OR)_2]$ [Por = TPP, R = $PhCH_2$ (1); Por = $(MeO)_{12}TPP$, R = Me (2), Et (3), $PhCH_2$ (4)]. To a solution of alcohol (two drops for benzyl alcohol; 2 mL for methanol or ethanol) in tetrahydrofuran (THF, 15 mL) was added $[Os(Por)(N_2)(THF)]$ (Por = TPP, $(MeO)_{12}$-TPP) (30 mg). The mixture was stirred for 0.5 h. The resulting red solution was evaporated to near dryness. The residue was then redissolved in dichloromethane (2 mL) and chromatographed on alumina using dichloromethane as the eluent. The leading brown band was collected and concentrated to ca. 2 mL. *n*-Heptane was then added to precipitate the product. Recrystallization from chloroform–heptane gave dark purple crystals (yield > 80%). Anal. Calcd for **1** ($C_{58}H_{42}N_4O_2Os$): C, 68.49; H, 4.16; N, 5.51. Found: C, 68.92; H, 4.32; N, 5.36. Calcd for **2** ($C_{58}H_{58}N_4O_{14}Os$): C, 56.85; H, 4.77; N, 4.57. Found: C, 56.38; H, 5.09; N, 4.99. Calcd for **3** ($C_{60}H_{62}N_4O_{14}Os$): C, 57.50; H, 4.99; N, 4.47. Found: C, 57.27; H, 4.80; N, 4.88. Calcd for **4** ($C_{70}H_{66}N_4O_{14}Os$): C, 61.03; H, 4.83; N, 4.07. Found: C, 60.99; H, 4.68; N, 4.31.

^1H NMR ($CDCl_3$) are as follows. **1** (270 MHz): H_β 4.15 (8H, s); H_o 9.34 (8H, m); H_m, Hp 8.22 (12H, m); $-OCH_2C_6H_5$ 6.32 (4H, tm) (H′m), 6.07 (2H, tm) (H′p), 1.77 (4H, d) (H′o); OCH_2Ph 32.39 (4H, s). **2** (90 MHz): H_β 4.83 (8H, s); H_o 8.49 (8H, s); *m*-OCH_3 4.17 (24H, s); *p*-OCH_3 4.44 (12H, s); Os–OCH_3 34.23 (6H, s). **3** (90 MHz): H_β 4.88 (8H, s); H_o 8.45 (8H, s); *m*-OCH_3 4.19 (24H, s); *p*-OCH_3 4.43 (12H, s); OCH_2CH_3 29.60 (4H, q); $-OCH_2CH_3$ 4.88 (6H, t). **4** (270 MHz); H_β 4.24 (8H, s); H_o 8.59 (8H, s); *m*-OCH_3 4.22 (24H, s); *p*-OCH_3 4.48 (12H, s); $-OCH_2C_6H_5$ 6.35 (4H, tm) (H′m), 6.04 (2H, tm) (H′p), 1.77 (4H, d) (H′o); $-OCH_2Ph$ 31.34 (4H, s). UV–vis ($CHCl_3$) [λ_{max}/nm (log ϵ): **1** (1.28×10^{-5} M), 271 (4.63), 343 (4.74) sh, 394 (5.07), 510 (4.25); **2** (1.10×10^{-5} M), 278 (4.37), 354 (4.53) sh, 409 (4.88), 509 (4.00); **3** (1.6×10^{-5} M), 278 (4.51), 354 (4.68) sh, 410 (4.98), 510 (4.19); **4** (1.09×10^{-5} M), 274 (4.35), 350 (4.50) sh, 409 (4.82), 512 (3.97). IR (Nujol) ["oxidation state marker" band (cm^{-1})]: **1**, 1016; **2–4**, 1014.

The preparation and spectral data of $[Os(TPP)(OR)_2]$ (R = Et (**5**), $CH(CH_3)_2$ (**6**), Ph (**7**)) were reported previously.[1b] Crystals of **5–7** suitable for X-ray structure determinations were obtained by recrystallization from CH_2Cl_2–EtOH, CH_2Cl_2–THF–CH_3CN, and CH_2Cl_2–THF–MeOH, respectively.

Physical Measurements. UV–visible spectra were recorded on a Milton Roy Spectronic 3000 array spectrophotometer. Infrared spectra were obtained using a Nicolet 20 SXC FT-IR spectrometer ^1H NMR spectra

---

† University of Hong Kong.

‡ National Taiwan University.

(1) See for example: (a) Buchler J. W.; Smith, P. D. *Chem. Ber.* **1976**, *109*, 1465. (b) Che, C. M.; Leung, W. H.; Chung, W. C. *Inorg. Chem.* **1990**, *29*, 1841 and references cited therein.

(2) Antipas, A.; Buchler, J. W.; Gouterman, M.; Smith, P. D. *J. Am. Chem. Soc.* **1978**, *100*, 3015.

(3) Bozak, R. E.; Hill, C. L. *J. Chem. Educ.* **1982**, *59*, 36 and references therein.

(4) Buchler, J. W.; Smith, P. D. *Angew. Chem., Int. Ed. Engl.* **1974**, *13*, 745.

0020-1669/92/1331-5220$03.00/0

Table I. Crystal Data and Data Collection Procedures for $[Os(TPP)(OEt)_2]$ (**5**), $[Os(TPP)(OCH(CH_3)_2)_2]$ (**6**), and $[Os(TPP)(OPh)_2]$ (**7**)

compd	$[Os(TPP)(OEt)_2]$	$[Os(TPP)(OCH(CH_3)_2)_2]$	$[Os(TPP)(OPh)_2]$
formula	$C_{48}H_{38}H_4O_2Os$	$C_{50}H_{42}N_4O_2Os$	$C_{56}H_{38}N_4O_2Os$
fw	892.2	921.11	989.15
space group	$P2_1/c$	$P\bar{1}$	$P\bar{1}$
a, Å	9.858 (1)	9.812 (1)	10.253 (1)
b, Å	15.646 (4)	11.093 (1)	10.724 (1)
c, Å	13.137 (2)	11.656 (1)	11.958 (1)
α, deg		70.83 (1)	62.08 (1)
β, deg	106.94 (1)	76.08 (1)	68.55 (1)
γ, deg		62.06 (1)	79.30 (1)
V, Å^3	1938.3 (6)	1052.9	1081.1
Z	2	1	1
temp, °C	25	27	24
d(calcd), g/cm^3	1.53	1.453	1.519
abs coeff, cm^{-1}	33.4	30.7	30.0
R^a	0.031	0.025	0.024
$R_w{}^b$	0.023	0.030	0.029

[a] $R = \Sigma||F_o| - |F_o||/\Sigma|F_o|$. [b] $R_w = [w(|F_o| - |F_c|)^2|/\Sigma w|F_o|^2]^{1/2}$.

Table II. Final Positions and Isotropic Thermal Parametes (B_{eq})[a] for $[Os(TPP)(OEt)_2]$ (**5**)

atom	x	y	z	B_{eq}, Å^2
Os	0	0	0	2.76 (3)
N(1)	−0.0337 (6)	−0.1165 (3)	0.0591 (4)	3.0 (3)
N(2)	−0.1442 (6)	0.0548 (3)	0.0638 (4)	3.1 (3)
C(1)	−0.1323 (7)	−0.1337 (4)	0.1129 (5)	3.1 (4)
C(2)	−0.1319 (8)	−0.2238 (4)	0.1328 (5)	4.0 (4)
C(3)	−0.0345 (8)	−0.2606 (4)	0.0916 (5)	3.8 (4)
C(4)	0.0280 (8)	−0.1939 (4)	0.0454 (5)	3.0 (4)
C(5)	0.1273 (8)	−0.2053 (4)	−0.0090 (5)	3.2 (4)
C(6)	−0.1813 (8)	0.1407 (4)	0.0596 (5)	3.3 (4)
C(7)	−0.2844 (9)	0.1524 (5)	0.1161 (6)	4.5 (5)
C(8)	−0.3086 (8)	0.0739 (5)	0.1533 (6)	4.3 (4)
C(9)	−0.2233 (7)	0.0152 (5)	0.1197 (5)	3.2 (4)
C(10)	−0.2182 (7)	−0.0743 (4)	0.1431 (5)	3.2 (4)
C(11)	0.1763 (8)	−0.2949 (4)	−0.0204 (5)	3.5 (4)
C(12)	0.2600 (10)	−0.3389 (5)	0.0657 (6)	5.7 (5)
C(13)	0.2999 (11)	−0.4220 (5)	0.0516 (6)	6.9 (6)
C(14)	0.2538 (11)	−0.4620 (5)	−0.0432 (6)	6.8 (6)
C(15)	0.1728 (9)	−0.4185 (5)	−0.1288 (6)	5.2 (5)
C(16)	0.1339 (8)	−0.3360 (5)	−0.1174 (5)	3.9 (4)
C(21)	−0.3152 (8)	−0.1050 (4)	0.2045 (6)	3.5 (4)
C(22)	−0.4614 (9)	−0.1060 (6)	0.1582 (6)	5.6 (5)
C(23)	−0.5513 (8)	−0.1281 (6)	0.2198 (7)	6.2 (6)
C(24)	−0.4948 (9)	−0.1533 (5)	0.3222 (7)	5.6 (5)
C(25)	−0.3522 (9)	−0.1565 (5)	0.3669 (6)	5.0 (5)
C(26)	−0.2611 (8)	−0.1321 (5)	0.3090 (6)	4.4 (4)
O	0.1492 (5)	0.0192 (3)	0.1289 (3)	3.9 (3)
C(31)	0.1963 (12)	0.0946 (6)	0.1768 (8)	9.5 (7)
C(32)	0.3343 (11)	0.1054 (7)	0.2254 (11)	11.9 (9)

[a] $B_{eq} = {}^1/_3\Sigma i\Sigma_j B_{ij}(a_i{}^*a_j{}^*)(a_ia_j)$.

Table III. Final Positions and Isotropic Thermal Parameters (B_{eq})[a] for $[Os(TPP)(OCH(CH_3)_2)_2]$ (**6**)

atom	x	y	z	B_{eq}/Å^2
Os	0.000	0.000	0.000	2.446 (4)
O(1)	0.0001 (3)	−0.1636 (2)	−0.0210 (2)	3.41 (6)
N(1)	0.2105 (3)	−0.1155 (3)	0.0677 (2)	2.78 (7)
N(2)	0.1060 (3)	0.0305 (3)	−0.1737 (2)	2.98 (7)
C(1)	0.2379 (4)	−0.1793 (4)	0.1891 (3)	3.14 (8)
C(2)	0.4018 (4)	−0.2541 (4)	0.1948 (3)	4.0 (1)
C(3)	0.4723 (4)	−0.2375 (4)	0.0807 (3)	3.8 (1)
C(4)	0.3540 (4)	−0.1496 (3)	−0.0007 (3)	3.12 (8)
C(5)	0.3793 (4)	−0.1053 (4)	−0.1277 (3)	3.17 (8)
C(6)	0.2637 (4)	−0.0201 (4)	−0.2067 (3)	3.27 (9)
C(7)	0.2907 (4)	0.0306 (4)	−0.3368 (3)	4.1 (1)
C(8)	0.1519 (4)	0.1074 (4)	−0.3811 (3)	4.1 (1)
C(9)	0.0347 (4)	0.1075 (3)	−0.2799 (3)	3.12 (8)
C(10)	−0.1249 (4)	0.1754 (4)	−0.2876 (3)	3.18 (8)
C(11)	0.5443 (4)	−0.1568 (4)	−0.1832 (3)	3.24 (9)
C(12)	0.6440 (4)	−0.1098 (4)	−0.1679 (4)	4.3 (1)
C(13)	0.7982 (4)	−0.1615 (5)	−0.2187 (4)	4.9 (1)
C(14)	0.8498 (4)	−0.2558 (5)	−0.2863 (4)	4.6 (1)
C(15)	0.7529 (4)	−0.3032 (5)	−0.3029 (5)	5.5 (1)
C(16)	0.5988 (4)	−0.2535 (4)	−0.2520 (4)	4.6 (1)
C(17)	−0.1808 (4)	0.2536 (4)	−0.4124 (3)	3.60 (9)
C(18)	−0.2192 (8)	0.3945 (5)	−0.4541 (4)	6.9 (2)
C(19)	−0.2742 (8)	0.4694 (6)	−0.5689 (5)	7.7 (2)
C(20)	−0.2886 (5)	0.4024 (6)	−0.6391 (4)	6.0 (2)
C(21)	−0.2468 (6)	0.2628 (6)	−0.6011 (4)	6.6 (1)
C(22)	−0.1940 (5)	0.1878 (5)	−0.4862 (4)	5.5 (1)
C(23)	0.0510 (4)	−0.3006 (4)	0.0601 (3)	3.70 (9)
C(24)	−0.0886 (6)	−0.3346 (5)	0.1077 (6)	6.5 (1)
C(25)	0.1771 (7)	−0.4028 (5)	−0.0096 (6)	6.8 (2)

[a] $B_{eq} = {}^1/_3\Sigma i\Sigma_j B_{ij}(a_i{}^*a_j{}^*)(a_ia_j)$.

were measured on a JEOL Model FX-90Q spectrometer (90 MHz) or a JEOL LNM-GSX 270 FT NMR spectrometer (270 MHz), and the chemical shifts (δ, ppm) were reported relative to tetramethylsilane (TMS). Elemental analyses of newly prepared complexes were performed by Butterworth Laboratories Ltd.

X-ray Structure Determinations of 5–7. Diffraction measurements were made at room temperature on a Nonius CAD4 diffractometer with graphite-monochromated Mo Kα (0.710 73 Å) radiation. The data collection and processing parameters are summarized in Table I. All computations were performed on a Micro Vax II computer using the Enraf-Nonius SDP program. The structures were solved by conventional heavy-atom methods. The position of the Os atom was located at the crystallographic center of symmetry for all three compounds. The coordinates of all the remaining non-hydrogen atoms were determined from subsequent Fourier maps. All non-hydrogen atoms were refined anisotropically, and the hydrogen atoms were fixed in idealized positions (C–H = 0.95 Å) with assigned thermal parameters. At the end of the refinement, final difference Fourier maps showed residuals in the range of −0.55 to 0.65, −0.4 to 0.7, and −1.00 to 1.74 e Å^{-3} for **5–7**, respectively.

Final positional and equivalent isotropic thermal parameters are listed in Tables II–IV. Selected bond lengths and angles are listed in Table V–VII. Calculated hydrogen parameters and complete lists of bond lengths, bond angles, and anisotropic thermal parameters are included as supplementary material.

Computational Section

The molecular orbital calculation is based on the extended Huckel calculation (EHMO), using the program ICON.[5] The basis functions of C, O, N, and H are taken from the default values of the program. The basis function of Os is as follows: $H_{ii}(s) = -10.4$ eV, $\zeta(s) = 2.448$; $H_{ii}(p) = -5.26$, $\zeta(p) = 2.28$; $H_{ii}(d) = -12.42$, $\zeta_1(d) = 5.55$, coefficient = 0.65, $\zeta_2(d) = 2.41$, coefficient = 0.577.

Results and Discussion

Syntheses and Characterization of 1–4. Our previous work showed the reduction of $[Os(Por)(O)_2]$ with ascorbic acid in the presence of ROH offers a general synthetic route for $[Os(Por)(OR)_2]$.[1b] Buchler and co-workers observed that treatment of

---

[5] Howell, J.; Rossl, A.; Wallace, D.; Haraki, K.; Hoffmann, R. ICON Program for extended Huckel molecular orbital calculations. Quantum chemistry program exchange, University of Indiana, Bloomington, IN, 1977.

Table IV. Final Positions and Isotropic Thermal Parameters (B_{eq})[a] for [Os(TPP)(OPh)$_2$] (**7**)

atom	x	y	z	B_{eq}/Å^2
Os	0.000	0.000	0.000	2.852 (3)
O(1)	0.1150 (2)	0.1499 (2)	–0.1568 (2)	3.71 (4)
N(1)	0.1050 (2)	0.0088 (2)	0.1119 (2)	3.16 (5)
N(2)	0.1366 (2)	–0.1516 (2)	–0.0357 (2)	3.23 (5)
C(1)	0.0728 (3)	0.0945 (3)	0.1762 (2)	3.36 (6)
C(2)	0.1710 (3)	0.0643 (3)	0.2457 (2)	3.93 (6)
C(3)	0.2587 (3)	–0.0393 (3)	0.2259 (3)	3.81 (6)
C(4)	0.2183 (3)	–0.0754 (3)	0.1421 (2)	3.27 (6)
C(5)	0.2824 (3)	–0.1786 (3)	0.0990 (2)	3.26 (6)
C(6)	0.2467 (3)	–0.2109 (3)	0.0142 (2)	3.40 (6)
C(7)	0.3173 (3)	–0.3127 (3)	–0.0345 (3)	4.19 (7)
C(8)	0.2509 (3)	–0.3154 (3)	–0.1115 (3)	4.17 (7)
C(9)	0.1356 (3)	–0.2167 (3)	–0.1116 (2)	3.42 (6)
C(10)	0.0377 (3)	–0.1915 (3)	–0.1757 (2)	3.40 (6)
C(11)	0.3966 (3)	–0.2666 (3)	0.1536 (2)	3.57 (6)
C(12)	0.5338 (4)	–0.2244 (4)	0.0909 (4)	6.1 (1)
C(13)	0.6361 (4)	–0.3057 (5)	0.1462 (5)	7.6 (1)
C(14)	0.6021 (4)	–0.4261 (4)	0.2607 (4)	6.87 (9)
C(15)	0.4682 (5)	–0.4695 (5)	0.3231 (4)	6.8 (1)
C(16)	0.3640 (4)	–0.3895 (4)	0.2678 (4)	5.07 (9)
C(17)	0.0533 (3)	–0.2775 (3)	–0.2493 (2)	3.51 (6)
C(18)	0.1350 (5)	–0.2327 (3)	–0.3802 (3)	5.30 (9)
C(19)	0.1512 (5)	–0.3164 (4)	–0.4451 (3)	6.0 (1)
C(20)	0.0876 (4)	–0.4429 (3)	–0.3803 (3)	4.93 (7)
C(21)	0.0062 (4)	–0.4877 (3)	–0.2504 (3)	5.34 (8)
C(22)	–0.0119 (4)	–0.4052 (3)	–0.1849 (3)	4.82 (8)
C(23)	0.1891 (3)	0.1505 (3)	–0.2772 (3)	3.90 (7)
C(24)	0.1293 (4)	0.2018 (3)	–0.3773 (3)	4.72 (8)
C(25)	0.2064 (5)	0.2086 (4)	–0.5013 (4)	6.4 (1)
C(26)	0.3438 (6)	0.1688 (5)	–0.5285 (4)	7.7 (1)
C(27)	0.4069 (5)	0.1185 (5)	–0.4290 (5)	7.3 (1)
C(28)	0.3296 (4)	0.1089 (4)	–0.3037 (4)	5.5 (1)

[a] $B_{eq} = {}^1/{}^3\sum_i\sum_j B_{ij}(a_i{}^*a_j{}^*)(a_ia_j)$.

Table V. Selected Bond Distances (Å) and Bond Angles (deg) in [Os(TPP)(OEt)$_2$] (**5**)

Distances			
Os–O	1.915 (4)	Os–N(1)	2.046 (5)
Os–N(2)	2.038 (5)	O–C(31)	1.36 (1)
C(31)–C(32)	1.33 (1)		
Angles			
O–Os–Oa	179.9	N(1)–Os–N(1)a	180.0
N(1)–Os–N(2)	90.5 (2)	N(1)–Os–N(2)a	89.5 (2)
N(1)–Os–O	88.4 (2)	N(2)–Os–N(2)a	180.0
N(2)–Os–O	91.1 (2)	N(2)–Os–Oa	90.0 (2)
Os–O–C(31)	128.2 (5)	O–C(31)–C(32)	120 (1)

Table VI. Selected Bond Distances (Å) and Bond Angles (deg) in [Os(TPP)(OCH(CH$_3$)$_2$)$_2$] (**6**)

Distances			
Os–O(1)	1.909 (4)	Os–N(1)	2.042 (3)
Os–N(2)	2.040 (3)	O(1)–C(23)	1.422 (4)
C(23)–C(24)	1.519 (7)	C(23)–C(25)	1.511 (6)
Angles			
O(1)–Os–O(1)a	180	O(1)–Os–N(1)	91.6 (1)
O(1)–Os–N(1)a	88.4 (1)	O(1)–Os–N(2)	88.3 (1)
O(1)–Os–N(2)a	91.8 (1)	N(1)–Os–N(2)	90.7 (2)
N(1)–Os–N(2)a	89.3 (2)	Os–O(1)–C(23)	127.0 (3)
O–C(23)–C(24)	107.9 (3)	O–C(23)–C(25)	108.0 (3)
C(24)–C(23)–C(25)	112.6 (5)		

Table VII. Selected Bond Distances (Å) and Bond Angles (deg) in [Os(TPP)(OPh)$_2$] (**7**)

Distances			
Os–O(1)	1.938 (2)	Os–N(1)	2.042 (3)
Os–N(2)	2.038 (2)	O(1)–C(23)	1.357 (4)
C(23)–C(24)	1.381 (5)	C(24)–C(25)	1.375 (5)
C(25)–C(26)	1.358 (8)	C(26)–C(27)	1.401 (9)
C(27)–C(28)	1.379 (6)	C(28)–C(23)	1.391 (5)
Angles[a]			
O(1)–Os–O(1)a	180	O(1)–Os–N(1)	89.8 (1)
O(1)–Os–N(1)a	90.2 (1)	O(1)–Os–N(2)	92.0 (1)
O(1)–Os(N2)a	88.0 (1)	N(1)–Os–N(2)	90.6 (2)
N(1)–Os–N(2)a	89.5 (2)	Os–O(1)–C(23)	127.5 (2)
O(1)–C(23)–C(24)	120.6 (3)	O(1)–C(23)–C(28)	120.0 (3)

[a] C–C–C angles in the phenyl ring of the phenoxide ligand vary from 119.4 (4) to 120.7 (4)°.

[Os(OEP)(N$_2$)(THF)] with methanol readily afforded [Os(OEP)(OMe)$_2$].[4] This finding aroused our interest since it promises an alternative general method for the preparation of [Os(Por)(OR)$_2$]. We prepared two new dinitrogenosmium(II) porphyrins, [Os(Por)(N$_2$)(THF)] (Por = TPP, (MeO)$_{12}$TPP), which exhibit ν_{N-N} at 2063 and 2060 cm^{-1}, respectively, by treatment of [Os(Por)(O)$_2$] with hydrazine hydrate in THF under a nitrogen atmosphere. Both [Os(TPP)(N$_2$)(THF)] and [Os((MeO)$_{12}$TPP)(N$_2$)(THF)] were found to react quickly with methanol, ethanol, and benzyl alcohol in THF at room temperature to give the respective [Os(Por)(OR)$_2$] complexes with high isolated yields (>80%).

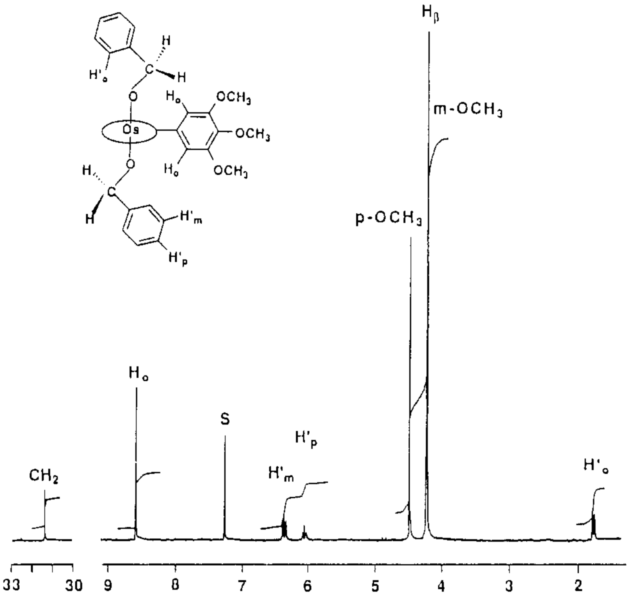

Figure 1. ^{1}H NMR spectrum of [Os(MeO)$_{12}$TPP)(OCH$_2$Ph)$_2$] (**4**) (CDCl$_3$, 270 MHz, TMS).

The complexes **1**–**4** show typical UV–visible spectra of [Os(Por)(OR)$_2$] as depicted elsewhere.[1b] The "oxidation state marker" bands appearing in their IR spectra are at 1016 cm^{-1} for **1** and 1014 cm^{-1} for **2**–**4**, in accordance with the Os(IV) formulation.[6,7] The ^{1}H NMR spectra of **1**–**4** show sharp lines for all proton resonances, but the methylene proton (Os–O–CH$_2$–) resonances of the alkoxide ligands are largely downfield shifted $\delta > 29$ ppm). Moreover, a large upfield shift was observed for the pyrrolic proton resonances (H$_\beta$) of the porphyrin ring. This indicates the paramagnetic nature of [Os(Por)(OR)$_2$]. All the other proton resonances also suffer paramagnetic shifts but to a much lesser extent. Figure 1 shows the ^{1}H NMR spectrum of **4**. In this 270-MHz spectrum, H$_\beta$ and the *m*-methoxy proton resonances nearly overlap. It is interesting to note that H'$_p$ appears at higher field than H'$_m$, which contrasts with the diamagnetic ruthenium(II), ruthenium(IV), and osmium(IV) porphyrins containing phenyl groups as the axial ligands.[8]

Structures of 5–7. The ORTEP drawings of **5**–**7** are shown in Figures 2–4, respectively. In the structures of these three

---

(6) Groves, J. T.; Ahn, K. H. *Inorg. Chem.* **1987**, *26*, 3833 and references therein.

(7) (a) Huang, J. S.; Che, C. M.; Poon, C. K. *J. Chem. Soc., Chem. Commun.* **1992**, 161. (b) Che, C. M.; Huang, J. S.; Li, Z. Y.; Poon, C. K. *Inorg. Chim. Acta* **1991**, *190*, 161.

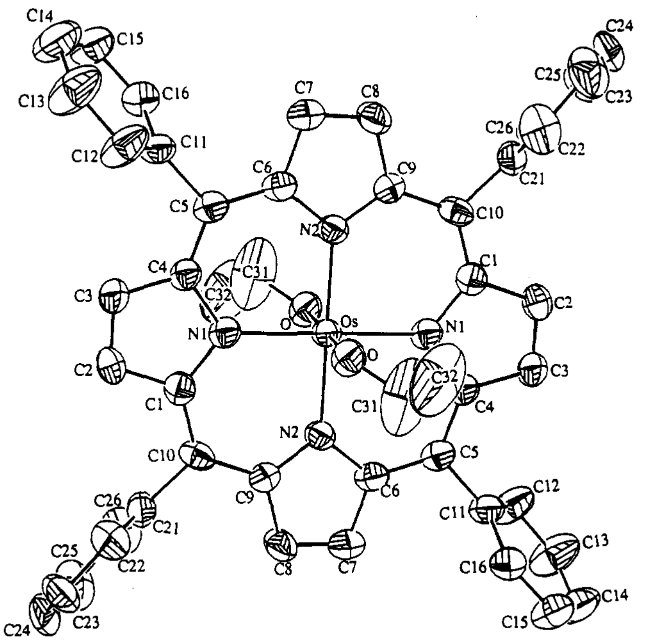

Figure 2. ORTEP drawing of $[Os(TPP)(OEt)_2]$ (**5**) with atomic labeling scheme.

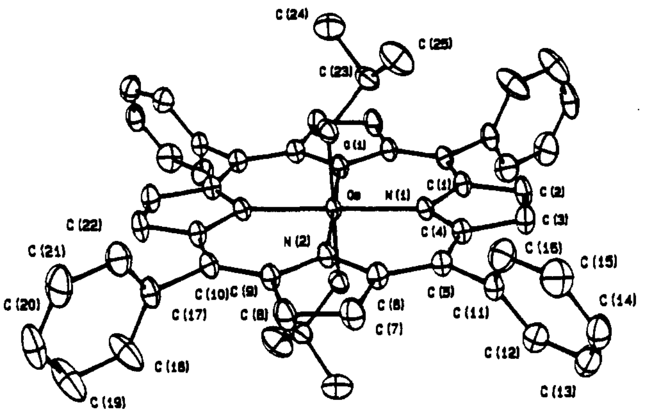

Figure 3. ORTEP drawing of $[Os(TPP)(OCH(CH_3)_2)_2]$ (**6**) with atomic labeling scheme. Thermal ellipsoids are drawn at the 30% probability level.

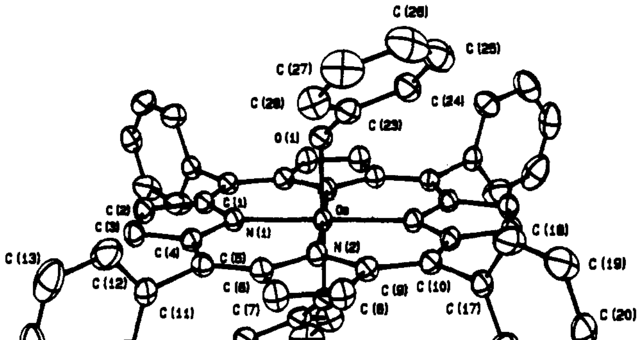

Figure 4. ORTEP drawing of $[Os(TPP)(OPh)_2]$ (**7**) with atomic labeling scheme. Thermal ellipsoids are drawn at the 30% probability level.

complexes, the Os atom is essentially in the porphyrin plane, which itself is slightly distorted. The four peripheral phenyl rings are approximately planar and nearly perpendicular to the porphyrin plane. For **7**, the dihedral angle between the phenoxide ring and the plane defined by the four pyrrolic nitrogen atoms is 42.8 (2)°. The O–Os–O axes in all the complexes **5**–**7** are required to be linear by symmetry (O–Os–O = 180°). These axes are close to being orthogonal to the porphyrin plane. Complexes **5**–**7** give nearly the same Os–O–C angles (127.0 (3)–128.2 (5)°), which are larger than the corresponding angle (120°) used in previous IEH calculations.[2]

The Os–OR distances of 1.915 (4), 1.909 (4), and 1.938 (2) Å for **5**–**7**, respectively, are shorter than a normal Os–O single bond (~2.1 Å), and this is attributed to $d\pi(Os)$–$p\pi(O)$ interaction. These distances are however significantly longer than the Os–O distance of 1.80 Å employed in previous IEH calculations.[2] The C–O bond distances of **5** and **7** (1.355 (11) and 1.357 (4) Å, respectively) are very similar, while this distance (1.429 (4) Å) is found to be slightly longer in **6**. Especially noteworthy is the C_{31}–C_{32} distance (1.33 (1) Å) of the ethoxy ligands in **5**, which is abnormally shorter than the expected value of ca. 1.5 Å for a C–C single bond. This unusual shortening may be due to the large thermal motions of both C atoms rather than a coordination effect since the corresponding C–C distances (1.511 (6)–1.519 (7) Å) in **6** are quite normal. The O–C–C angles of **5** and **6** are different (**5**, 120 (1)°; **6**, 107.9 (3)–108.0 (3)°), probably because of different steric effect resulting from their very different C–O bond lengths.

The structures of osmium porphyrins reported in the literature are sparse, including $[Os(OEP)(OMe)]_2O$,[9] $[Os(OEPMe_2)(CO)(Py)]$,[10a] $[Os(TPP)(OPPh_3)_2]$,[10b] $[Os(TPP)(PPh_3)_2]$,[10b] $[Os(TTP)(O)_2]$,[10c] and $[Os(OEP)(O)_2]\cdot C_6H_5Cl$.[10d] Table VIII compares the averaged values of the structural parameters in the porphyrin skeleton for **5**–**7** and the related dimeric alkoxyosmium(IV) and -ruthenium(IV) porphyrins. These structural parameters for **5**–**7** show no unusual features when compared with those of the (μ-oxo)alkoxyosmium(IV) and -ruthenium(IV) dimers as well as other monomeric osmium and ruthenium porphyrins.[8,9,10b,11]

The shorter Os–OR distances in **5**–**7** as noted above suggest strong RO–Os π-bonding. Although such a bonding interaction also exists in a (μ-oxo)osmium(IV) dimer such as $[Os(OEP)(OMe)]_2O$, the latter complex,[12] like its ruthenium analogue,[11] is diamagnetic. This diamagnetism can be understood on the basis of an ordering for the metal d orbitals of an $(MN_4)_2O$ unit developed by Tatsumi and co-workers[13] or a qualitative energy diagram shown by Masuda and co-workers.[14] In the present work, the paramagnetic nature of the monomeric [Os(Por)(OR)$_2$] is not unusual for a d^4 ion having significant metal–ligand π-bonding, because the d_{xz} and d_{yz} orbitals are destabilized relative to d_{xy} through metal–oxygen π-bonding. However, something important should be considered. Qualitatively, the solid structures of **5**–**7** have symmetry lower than D_{4h}, which splits the d_{xz} and d_{yz} orbitals of osmium if the z axis is defined to lie along the RO–Os–OR axis. However, this splitting, which is due to the bending of Os–O–R axis, should be small, since the OsN_4O_2 moiety in the structures of **5**–**7** is only slightly distorted from an octahedron of D_{4h} symmetry. This has also been suggested

---

(8) (a) Groves, J. T.; Ahn, K. H.; Quinn, R. *J. Am. Chem. Soc.* **1988**, *110*, 4217. (b) James, B. R.; Pacheco, A.; Rettig, S. J.; Ibers, J. A. *Inorg. Chem.* **1988**, *27*, 2414. (c) Huang, J. S.; Che, C. M.; Li, Z. Y.; Poon, C. K. *Inorg. Chem.* **1992**, *31*, 1313. (d) Che, C. M.; Huang, J. S.; Li, Z. Y.; Poon, C. K. Unpublished results.

(9) Masuda, H.; Taga, T.; Osaki, K.; Sugimoto, H.; Mori, M. *Bull. Chem. Soc. Jpn.* **1984**, *57*, 2345.

(10) (a) Buchler, J. W.; Lay, K. L.; Smith, P. D.; Scheidt, W. R.; Rupprecht, G. A.; Kenny, J. E. *J. Organomet. Chem.* **1976**, *110*, 109. (b) Che, C. M.; Lai, T. F.; Chung, W. C.; Schaefer, W. P.; Gray, H. B. *Inorg. Chem.* **1987**, *26*, 3907. (c) Che, C. M.; Chung, W. C.; Lai, T. F. *Inorg. Chem.* **1988**, *27*, 2801. (d) Nasri, H.; Scheidt, W. R. *Acta Crystallogr.* **1990**, *C46*, 1096.

(11) Collman, J. P.; Barnes, C. E.; Brothers, P. J.; Collins, T. J.; Ozawa, T.; Gallucci, J. C.; Ibers, J. A. *J. Am. Chem. Soc.* **1984**, *106*, 5151.

(12) Sugimoto, H.; Higashi, T.; Mori, M.; Nagano, M.; Yoshida, Z.-i.; Ogoshi, H. *Bull Chem. Soc. Jpn.* **1982**, *55*, 822.

(13) (a) Tatsumi, K.; Hoffmann, R. *J. Am. Chem. Soc.* **1981**, *103*, 3328. (b) Tatsumi, K.; Hoffmann, R.; Whangbo, M.-H. *J. Chem. Soc., Chem. Commun.* **1980**, 509.

(14) Masuda, H.; Taga, T.; Osaki, K.; Sugimoto, H.; Mori, M.; Ogoshi, H. *J. Am. Chem. Soc.* **1981**, *103*, 2199.

Table VIII. Averaged Bond Lengths (Å) and Angles (deg) for the Porphyrin Core of Monomeric and Dimeric Alkoxyosmium(IV) and -ruthenium(IV) Porphyrins

length or angle	$[Os(OEP)(OMe)]_2O$[9]	$[Ru(TPP)(p\text{-}O\text{-}Tol)]_2O$[11]	$Os(TPP)(OPr^i)_2$ (6)[b]	$Os(TPP)(OPh)_2$ (7)	$Os(TPP)(OEt)_2$ (5)
Os (Ru)–N	2.033 (35)	2.050 (14)	2.041 (3)	2.040 (3)	2.042 (5)
$N–C_a$[a]	1.37 (6)	1.375 (23)	1.384 (4)	1.382 (4)	1.382 (9)
$C_a–C_m$	1.39 (7)	1.391 (23)	1.394 (5)	1.390 (5)	1.400 (10)
$C_m–C_p$		1.497 (22)	1.503 (5)	1.502 (5)	1.501 (10)
$C_a–C_b$	1.47 (7)	1.436 (24)	1.435 (5)	1.433 (5)	1.426 (10)
$C_b–C_b$	1.37 (7)	1.352 (23)	1.343 (5)	1.345 (6)	1.364 (11)
$C_a–N–C_a$	106 (3)	108.0 (15)	107.0 (3)	107.2 (3)	106.6 (6)
$N–C_a–C_b$	109 (4)	108.3 (17)	108.6 (3)	108.6 (4)	109.3 (6)
$N–C_a–C_m$	125 (4)	126.3 (18)	125.8 (3)	125.8 (4)	125.7 (6)
$C_a–C_b–C_b$	107 (4)	107.6 (18)	107.9 (3)	107.8 (4)	107.4 (6)
$C_a–C_m–C_a$	126 (4)	124.9 (18)	125.4 (4)	125.5 (4)	125.3 (6)
$C_a–C_m–C_p$		117.5 (16)	117.3 (3)	117.3 (4)	117.3 (6)

[a] The symbols C_a and C_b are defined as the carbon atoms α and β to the pyrrole N, respectively. C_m and C_p refer to the respective meso and phenyl carbon atoms bonded to the porphyrin ring. [b] $Pr^i = CH(CH_3)_2$.

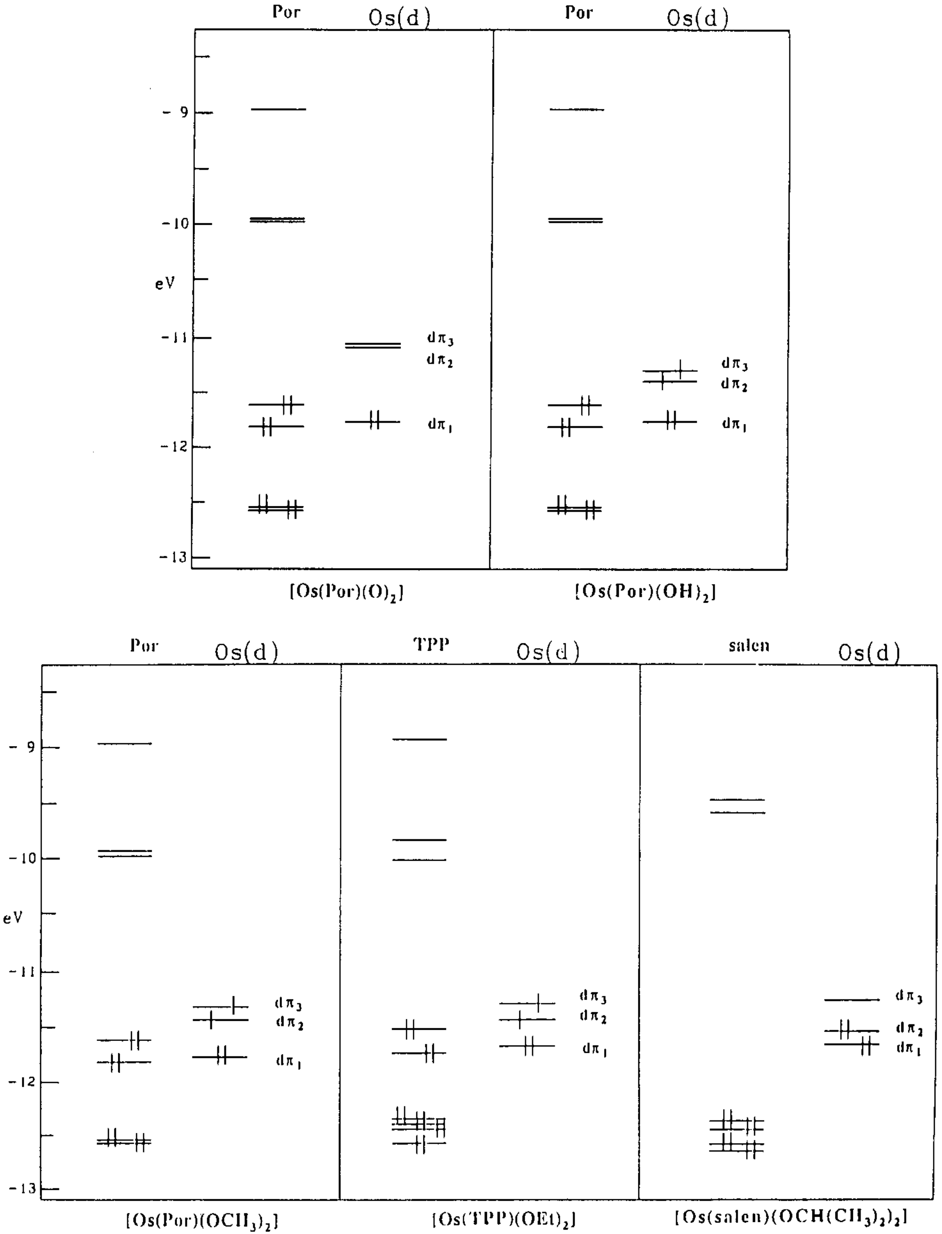

Figure 5. Energies of top filled and lowest empty MOs for $[Os(TPP)(OEt)_2]$ (5), $[Os(salen)(OCH(CH_3)_2)_2]$, and other related osmium porphyrins.

previously[2] and reconfirmed by the present calculation as discussed later. On the other hand, the RO–Os π-bonding is expected to destablize the $d\pi_2$ and $d\pi_3$ orbitals (here the $d\pi_1$ orbital contains mainly the d_{xy} character, whereas $d\pi_2$ and $d\pi_3$ contain mainly d_{xz} and d_{yz}) to nearly the same extent considering that both p_x and p_y electron pairs of oxygen contribute to this π-bonding. Thus, the energy gap between the $d\pi_2$ and $d\pi_3$ orbitals would be so small that the ground state for the Os(IV) ion (d^4) is predicted to be a triplet of the configuration $(d\pi_1)^2(d\pi_2)^1(d\pi_3)^1$. On the other hand, if the symmetry of dialkoxyosmium(IV) is lowered to an extent that a large energy gap between $d\pi_2$ and $d\pi_3$ exists, a singlet $((d\pi_1)^2(d\pi_2)^2$ ground state may be expected. Such may be the case when the equatorial porphyrinato ligand is replaced by a less symmetrical one such as *N,N'*-ethylenebis(salicyclideneaminate) (salen). The observed very low μ_{eff} value of 1.1 μ_B for [Os(salen)(OCH(CH$_3$)$_2$)$_2$][15b] may be due to such reasoning. In order to confirm this, we have performed calculations on several Os complexes based on the EHMO as in the earlier calculation.[2] In this calculation, we include five compounds from an exact D_{4h} [Os(Por)(O)$_2$] to a much lower symmetry complex of [Os(salen)(OCH(CH$_3$)$_2$)$_2$].[15] The electronic states near the HOMO of these five compounds are displayed in Figure 5 to illustrate the relationship between the local symmetry of Os and the energy gap of the dπ_2 and dπ_3 orbitals. It is apparent that in [Os(Por)(O)$_2$] (D_{4h}) these two orbitals are degenerate. When two axial oxo ligands are replaced by a hydroxy group (with H-atom located at 45° from the *xz* plane), the two orbitals are split with a small gap of 0.10 eV. This gap becomes slightly bigger (0.112 eV) with the two axial ligands replaced by a $-OCH_3$ group. Complex **5** gives a gap of 0.123 eV, and last, [Os(salen)(OCH(CH$_3$)$_2$)$_2$] gives a gap of 0.296 eV. The calculations on [Os(TPP)(OEt)$_2$] (**5**) and [Os(salen)(OCH(CH$_3$)$_2$)$_2$][15b] are based on the measured bond distances and angles, and the result clearly indicated a much smaller gap between the dπ_2 and dπ_3 orbitals in **5**. This may explain the low μ_{eff} value of [Os(salen)(OCH(CH$_3$)$_2$)$_2$].[15] From such systematic studies, we conclude that the degeneracy of the dπ_2 and dπ_3 orbitals is mainly dependent on the local symmetry of the equatorial ligand in the dialkoxyosmium(IV) complexes.

Acknowledgment. This research was supported by the Hong Kong Research Grants Council and the University of Hong Kong. C-M.C. thanks the National Science Council of Taiwan for a Visiting Professorship.

Supplementary Material Available: Tables S1–S10, listing crystal data and details of the structure determination, atomic coordinates, hydrogen atom parameters, anisotropic thermal parameters, and bond distances and angles (11 pages). Ordering information is given on any current masthead page.

---

[15] (a) Che, C. M.; Cheng, W. K.; Mak, T. C. W. *Inorg. Chem.* **1986**, *25*, 703. (b) Cheng, W. K.; Che, C. M.; Wong, K. Y.; Tong, W. F.; Lai, T. F. *J. Chem. Soc., Dalton Trans.* **1992**, 91.